

Anomalous phase in one-dimensional, multilayer, periodic structures with birefringent materials

A. Mandatori, C. Sibilia,* and M. Bertolotti

INFN at Dipartimento di Energetica, Università "La Sapienza" di Roma, Via Scarpa 16, 00161 Rome, Italy

S. Zhukovsky

Institute of Molecular and Atomic Physics, National Academy of Sciences of Belarus, Minsk, Belarus

J. W. Haus

Electro-Optics Program, University of Dayton, Dayton, Ohio 45469-0245, USA

M. Scalora

U.S. Army Aviation and Missile Command, Weapon Sciences Directorate, AMSMI-RD-WS-ST Redstone Arsenal, Huntsville, Alabama 35898-5000, USA

(Received 11 March 2004; published 15 October 2004)

We have studied biaxial, birefringent, one-dimensional, multilayer structures and found a wavelength region where the phase of one specific polarization component of the transmitted field increases with wavelength, giving rise to unusual polarization dependent dispersive effects of the input beam. We discuss the conditions that lead to these effects, and examine possible ways to enhance them.

DOI: 10.1103/PhysRevB.70.165107

PACS number(s): 42.70.Qs, 42.25.Lc, 42.30.Lr

I. INTRODUCTION

Multilayer and photonic band-gap structures have many interesting characteristics due to their inherent dispersion properties. An example is presented in Ref. 1, where it is discussed how to design thin-film multilayer structures that separate multiple wavelength channels with a single stack by spatial dispersion, thus allowing compact, manufacturable wavelength multiplexers and demultiplexers, beam steering, dispersion-control devices, and superprism phenomena.

Extraordinary angle-sensitive light propagation, called *superprism phenomenon*, was demonstrated at optical wavelength in three-dimensional (3D) photonic crystals fabricated on Si substrate;² this effect together with wavelength sensitivity is at least two orders of magnitude stronger than that of the conventional prism. In Ref. 2 the incident-angle dependence including negative refraction and multiple beam branching was interpreted from highly anisotropic dispersion surfaces derived by photonic band calculation.

Recently, it has also become clear that dielectric structures with periodic variations on the scale of wavelength, i.e., photonic crystals,³⁻⁵ may enable anomalous refraction behavior^{2,6-8} giving rise to negative refraction of light similar to the one predicted for left-handed materials.⁹⁻¹¹ The physical principles behind these unusual phenomena in photonic crystals are based on complex Bragg scattering, and are very different from those in a left-handed metamaterial. For example, both negative refraction and subwavelength imaging may be realized in photonic crystals *without* employing a negative index or a backward wave.^{7,8} Photonic crystals thus represent another class of metamaterial with electromagnetic properties not available in a conventional medium.^{12,13}

In this paper we will show that in the case of one-dimensional, multilayer photonic crystal structures suitably constructed with birefringent layers, the phase of one specific polarization component of the transmitted field anomalously

increases with wavelength, giving rise to unusual polarization-dependent, dispersive effects on the input beam. When this occurs, the result may be an anomalous spatial shift of the output beam, qualitatively reminiscent of the kinds of shifts predicted for negative refractive index materials,¹⁰ and negative bending as demonstrated for superprism phenomena in 3D photonic crystals,² although at expenses of the energy of the transmitted field. More recently *amphoteric refraction* (the ability to refract light and ballistic electrons without reflections) has been reported for a class of birefringent materials that appears to be readily available, that have both positive permittivity and permeability.¹⁴ The index of refraction is matched on both sides of the interface, and material growth techniques allow for the identification of a reflection symmetry plane, with 0% reflections losses, giving rise to unusual transmission effects.

In what follows we study birefringent, multilayer, periodic structures in the optical domain, in a wavelength range that shows the presence of an anomalous phase change as a function of wavelength in the transmission and reflection spectra. With the term anomalous phase here we mean that the coefficient of transmission displays a phase with positive slope as a function of wavelength. Thus one can infer that anomalous dispersive effects occur inside the structure as the electromagnetic energy is redistributed between the different polarization components, which lead to the spatial filtering and *anomalous shifts* in the direction of propagation. This behavior is found by applying the transfer-matrix method,¹⁵ which we simplify here by applying a ray tracing method.

The energy exchange mechanism between the two polarization channels permitted by the birefringent materials and the difference in optical paths conspire to generate the anomalous phase which causes the center of gravity of the beam to undergo a spatial anomalous shift away from the refraction angle. The explanation of the beam shift associated with a temporal translation in advance of the wave front,

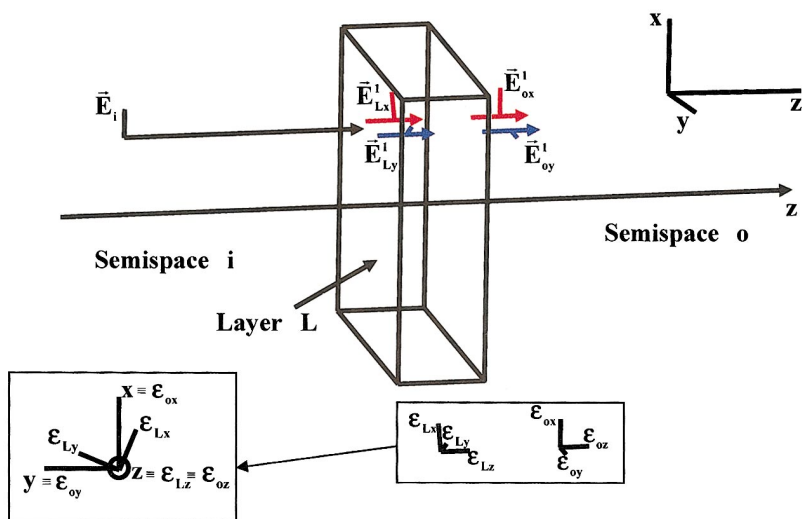


FIG. 1. (Color) Representation of the field inside and outside the anisotropic layer. The two electric fields inside the layer are the fields in the two channels of the anisotropic material. The input semispace is isotropic while the output semispace is anisotropic.

at a given polarization, is also presented. Although the predicted shift in the proposed example appears to be rather small, $\approx 1/\mu\text{m}$, conditions may exist that would favor its further enhancement by using crystals grown as pointed out in Ref. 14.

II. RAY METHOD TO STUDY ANISOTROPIC MEDIUM

To study one-dimensional layered structures different mathematical methods have been developed. One of the most often used methods is based on the transfer matrix, which effectively solves the Helmholtz equation, and arrives at a product of matrices from which transmission, reflection, and fields can be obtained with the help of a computer.^{16,17} One method that provides a direct link with the physical nature of the system is the ray method. Each ray is followed as it is transmitted and reflected at each interface. Then, summing up all contributions from each interface with the proper phase it provides quantities of interest, such as transmission, reflection, and the field and its phase.

The propagation of each ray inside an isotropic material is easy to follow and define mathematically. The problem is naturally more difficult if the material is anisotropic, because every wave is divided into two waves of different polarizations. However, the ray method can also be extended to this case, with some modifications. In the present paper we present results that arise from an anomalous development of the phase of the field. If we consider the phase of the transmission coefficient of an isotropic, strictly periodic and lossless multilayer structure, in most cases one would find that the phase is a monotonically decreasing function of wavelength. Here we report that for the case of a structure composed of anisotropic layers there is a range of wavelengths in which the slope of the phase is positive, and therefore anomalous. We therefore expect anomalous propagation effects to follow.

Here we apply the ray method to discuss the reason of the anomalous phase. The results even if not shown here are consistent with matrix method.^{15,16} Although the anomalous phase can be obtained also in two- and three-dimensional structures, for simplicity we limit our discussion to one-

dimensional, anisotropic, multilayered structures.

Let us consider the simple situation represented in Fig. 1, where one birefringent layer is placed between two semispaces, one isotropic (at the left, on the side of the incoming beam) and the *other anisotropic* (at the right, at the output side). An input plane wave is shown with linear polarization along the x direction, propagating along the z direction. The birefringent material (L) has the crystal axis as represented in the figure, rotated by some angle around the z direction. The wave is divided into two independent, linearly polarized plane waves travelling along z , with orthogonal electric fields along the axes labeled x_L and y_L . In terms of rays one may argue that these waves are the result of the transmission of the incident ray that passes through the interface between the incident-wave semispace i and the layer L . Two waves, with different velocities, propagate inside the layer L and reaching the interface with the output-wave semispace to generate two transmitted waves and two reflected waves (the latter ones not shown for simplicity). The subscripts in the symbols of the electric field indicate the medium in which the rays propagate and the component of the electric field with respect to the axis of the medium. The superscript denotes the ray associated with a particular path (in the figure there is only the number “one” because we are referring to the first traversal ray inside the layer and at the output; other rays with multiple reflections at each boundary would be successively numbered).

The transmitted and reflected field amplitudes at each interface are related to the input ray amplitude by the matrix relation

$$\vec{E}_L^1 = \alpha_{iL} \vec{E}_i,$$

$$\vec{E}_r^1 = \beta_{iL} \vec{E}_i, \tag{1}$$

where $E_i = E_{ix}$ is the incoming field and the transmitted and reflected amplitudes are

$$\vec{E}_L^1 = \begin{pmatrix} E_{Lx}^1 \\ E_{Ly}^1 \end{pmatrix}; \quad \vec{E}_i^1 = \begin{pmatrix} E_{ix}^1 \\ E_{iy}^1 \end{pmatrix}, \quad (2)$$

respectively. With reference to Fig. 1 and using the ray method we can soon find the analytical expression of the first transmitted ray across the slab as

$$\vec{E}_o^1 = \alpha_{Lo} \Delta \alpha_{iL} \vec{E}_i^1, \quad (3)$$

where Δ is the matrix that represents the propagation inside the birefringent layer L

$$\Delta = \begin{pmatrix} e^{ik_{Lx}d} & 0 \\ 0 & e^{ik_{Ly}d} \end{pmatrix}, \quad (4)$$

where d is the thickness of layer L . We write Eq. (3) in a more explicit way to obtain

$$\begin{pmatrix} E_{ox}^1 \\ E_{oy}^1 \end{pmatrix} = \begin{pmatrix} \alpha_{Lo}^{11} & \alpha_{Lo}^{12} \\ \alpha_{Lo}^{21} & \alpha_{Lo}^{22} \end{pmatrix} \begin{pmatrix} e^{ik_{Lx}d} & 0 \\ 0 & e^{ik_{Ly}d} \end{pmatrix} \begin{pmatrix} \alpha_{iL}^{11} & \alpha_{iL}^{12} \\ \alpha_{iL}^{21} & \alpha_{iL}^{22} \end{pmatrix} \begin{pmatrix} E_i \\ 0 \end{pmatrix}, \quad (5)$$

which yields the relation

$$\begin{pmatrix} E_{ox}^1 \\ E_{oy}^1 \end{pmatrix} = \begin{pmatrix} (\alpha_{iL}^{11} \alpha_{Lo}^{11} e^{ik_{Lx}d} + \alpha_{iL}^{21} \alpha_{Lo}^{12} e^{ik_{Ly}d}) E_i \\ (\alpha_{iL}^{11} \alpha_{Lo}^{21} e^{ik_{Lx}d} + \alpha_{iL}^{21} \alpha_{Lo}^{22} e^{ik_{Ly}d}) E_i \end{pmatrix}. \quad (6)$$

This is the exact expression of the transmitted field due to the first traversal ray when the input consists of a plane wave with linear polarization along the x direction, as represented in Fig. 1. This of course is not the total transmitted field, but only the first traversal of the slab; it is then necessary to superpose an infinite number of contributions from successive multiple reflections of the waves with the proper phase in order to obtain the total field at the output.

As Eq. (6) suggests, at the output we will have two plane waves with linear orthogonal polarizations that propagate independently of one another. The anomalous phase can exist for both polarization channels, although not in the same wavelength range. To explain this phenomenon we make reference only to the channel ε_{ox} . We can see immediately from Eq. (6) that the first transmitted ray is obtained by summing two complex terms, as shown in the complex plane in Fig. 2. The two vectors in the sum rotate with different velocities. For simplicity we now assume that $k_{Lx} = 2\pi n_{Lx}/\lambda_0 < k_{Ly} = 2\pi n_{Ly}/\lambda_0$ ($n = \sqrt{\varepsilon}$). In this case the first vector in the sum $V_1 = \alpha_{iL}^{11} \alpha_{Lo}^{11} e^{ik_{Lx}d}$ rotates in the complex plane at a lower rate than the second vector $V_2 = \alpha_{iL}^{21} \alpha_{Lo}^{12} e^{ik_{Ly}d}$. The summation of the two vectors will rotate around the center of the coordinate axis and its phase will be approximately the phase of the total output field. The *anomalous phase* is due to the difference of velocity between the two vectors V_1 and V_2 , and from the difference in the length of the vectors. In fact if the faster vector were longer than the slower vector, the anomalous phase could not occur for any velocity of rotation of the fast vector. To consider only the two vectors V_1 and V_2 is only a first approximation, but it is good enough to satisfactorily explain the generation of the anomalous phase. All other contributions rotate in the complex plane with frequencies that are multiples of the frequency of rotation of the two main vectors represented in Fig. 2; their amplitudes become

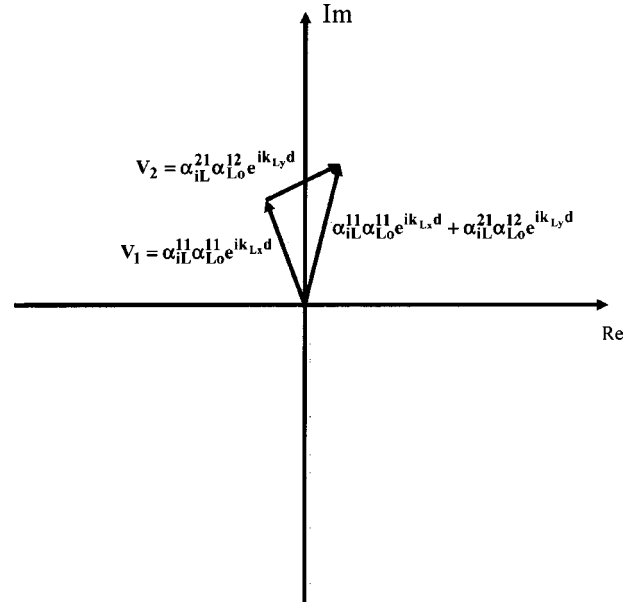


FIG. 2. Representation in the complex plane of the sum of the electric fields of the two channels of the anisotropic semispace in output. The sum is referred to the first ray in output only.

smaller and smaller, and therefore, the anomalous phase that we observe in the first ray at the output will be observed also in the spectrum of the total field and the physical explanation of the phenomena is just the same.

Inspection of Fig. 2 and Eq. (6) suggests that *in order to have anomalous phase* it is necessary that on both the channels, V_1 and V_2 , the electric fields have comparable amplitude. This means that the energy should be nearly equally split between the two paths, provided that the field component with the longer optical path has a slightly smaller amplitude. This can be achieved when the optical axis of one of the two birefringent media is rotated of about 40° – 45° with respect to the other one, and when optical paths between two channels are nearly equal.

Now we wish to understand how a multilayer structure modifies the process of generation of the anomalous phase. For this we will slightly complicate the structure represented in Fig. 1 by inserting another anisotropic layer and by analyzing this system using ray theory (Fig. 3). We have now two anisotropic layers A and B between two semispaces (anisotropic semispace o for the output and isotropic semispace i for the input). We assume that the crystals of the two materials A and B are rotated with respect to each other. In this case the first ray at the input of layer B is found by summing an infinite number of rays transmitted from multilayer A . Using the same notation as in Eq. (3), we can write the expression for the first transmitted ray at the output semispace

$$\vec{E}_o^1 = \alpha_{bo} \Delta_b \alpha_{ab} [I - \Delta_a \beta_{ai} \Delta_a \beta_{ab}]^{-1} \Delta_a \alpha_{ia} \vec{E}_i^1, \quad (7)$$

where I is the unitary matrix $I = \begin{pmatrix} 1 & 0 \\ 0 & 1 \end{pmatrix}$. We define a matrix M as

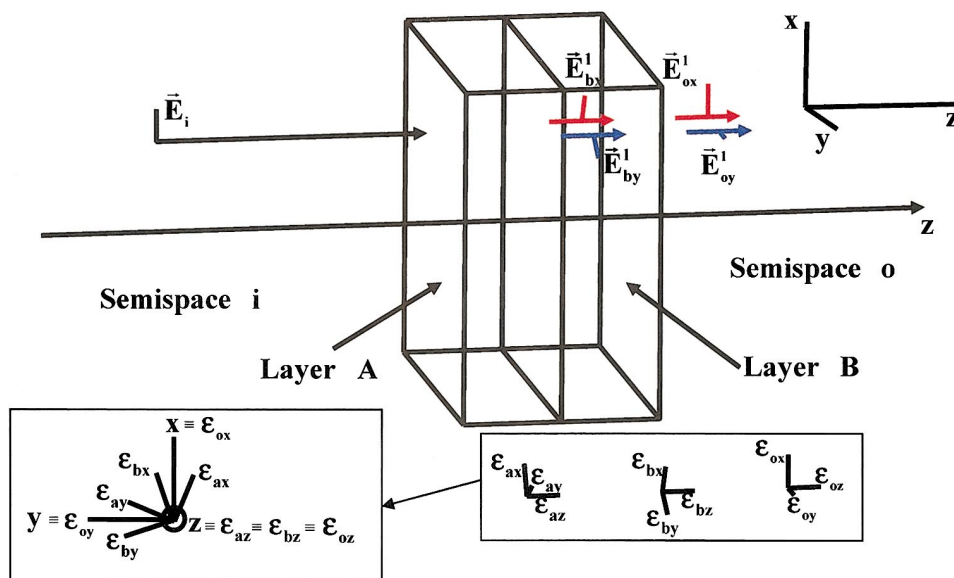


FIG. 3. (Color) Representation of the field that is inside and outside two anisotropic layers.

$$M = \alpha_{ab} [I - \Delta_a \beta_{ai} \Delta_a \beta_{ab}]^{-1} \Delta_a \alpha_{ia}. \quad (8)$$

The matrix M is the transmission matrix for a Fabry-Perot formed by the semispace i from which the incident wave arrives, the central layer A and the material B that is at the output of the wave. The elements of the matrix M have a functional dependence on the wavelength; all the considerations about the anomalous phase that apply to the single slab system in Fig. 1 are also valid for the elements of this matrix. Equation (7) can be written in a more compact way as

$$\vec{E}_o^1 = \alpha_{bo} \Delta_b M \vec{E}_i, \quad (9)$$

and expanding Eq. (9) and considering that the field in input is polarized along the x axis, we obtain

$$\begin{pmatrix} E_{ox}^1 \\ E_{oy}^1 \end{pmatrix} = \begin{pmatrix} [M_{11} \alpha_{bo}^{11} e^{ik_{bx}d} + M_{21} \alpha_{bo}^{12} e^{ik_{by}d}] E_i \\ [M_{11} \alpha_{bo}^{21} e^{ik_{bx}d} + M_{21} \alpha_{bo}^{22} e^{ik_{by}d}] E_i \end{pmatrix}. \quad (10)$$

The similarities between Eq. (10) and Eq. (6) are apparent. The vectors in the complex plane can have an anomalous phase that sum to the phase of the corresponding exponentials in Eq. (10). This shows that a multilayer structure usually does not change the phenomenon of the generation of the anomalous phase. Instead, it seems to propagate the effect along through the interference phenomena inside each layer. Moreover, a change of value of the rotation angle among the optical axis of the crystal or the refractive index values can cause a wavelength shift of the anomalous phase region. In the Appendix A we give the conditions that the parameters of a multilayer structure have to fulfil in order to obtain anomalous phase.

The anomalous phase displays interesting temporal and spatial characteristics, because if we speak in terms of the (spatial and temporal) Fourier transform of the field and remember that a transmission coefficient with a linear phase, negative slope, and constant amplitude gives a delay in time and a spatial shift in space, then we can immediately conclude that for a field tuned within the anomalous phase's

spectral region the output beam will be advanced in time rather than being delayed or shifted in a direction opposite to that expected from Snell's law with positive refractive index. This superluminal-like phenomenon does not contradict the principle of causality because there is a concomitant energy loss in the forward direction yielding small transmission values. In short, the larger the slope of the anomalous phase is, then the larger the time advance of a pulse or the spatial shift of the transverse profile will be (see Appendix B).

III. EXAMPLES

We report in this section some examples that better clarify the analytical results discussed previously. We study a system as represented in Fig. 1. All the results have been compared with result obtained using the matrix method,¹⁷ and found them to be consistent with ours. The input wave enters normally with linear polarization along the x axis. The dielectric index of the isotropic material in input is $\epsilon_i=1$ while the material that constitutes the central layer has dielectric indices $\epsilon_{Lx}=1.8$, $\epsilon_{Ly}=3.7$, $\epsilon_{Lz}=2.0$, and the output anisotropic material has the dielectric tensor with eigenvalues $\epsilon_{ox}=3.0$, $\epsilon_{oy}=1.7$, $\epsilon_{oz}=2.0$. The crystal of the central layer is rotated by 40° around the z axis, while the crystal of the material at the output has the principal axis directed along the directions of the Cartesian axis of the input material. In the graphs of Fig. 4 the phase of the output wave polarized along the x direction (from the channel ϵ_{ox}) is analyzed. Figure 4(a) refers to the first ray at the output as reported in Eq. (6). In the graph of the phase a small anomalous behavior in the phase is evident in the range of wavelengths between 3.5 and $4 \mu\text{m}$. Figure 4(b) represents the phase of the wave obtained as a sum of the first and the second output ray, which suggests that the anomalous phase amplifies; this means that the contribution of the second ray is strong enough to modify the phase. In Fig. 4(c) the phase for the wave obtained as a sum of the first three output rays is shown. The figure is similar to Fig. 4(b); already the contri-

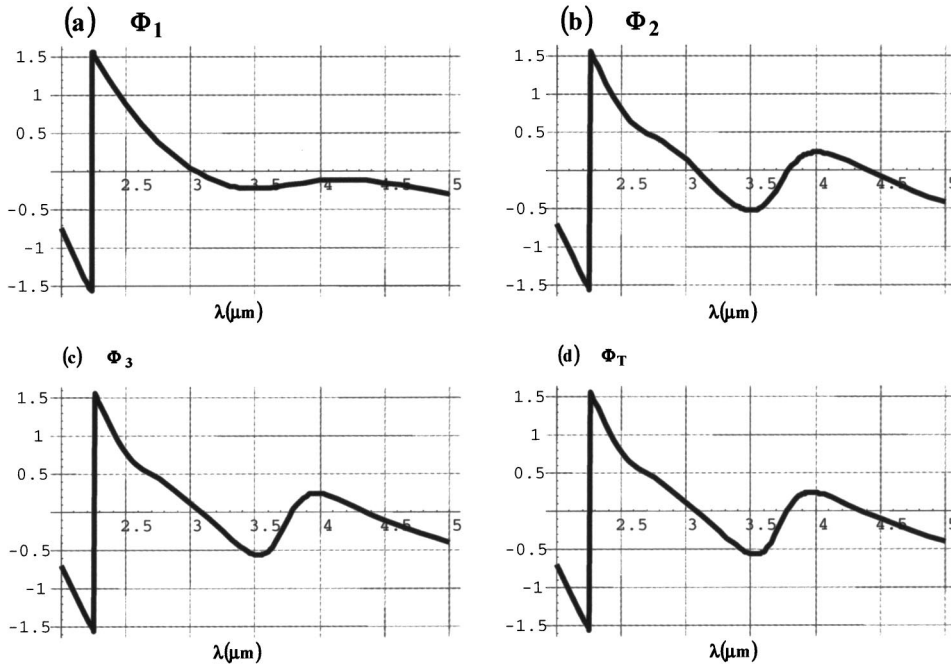


FIG. 4. The phase of the wave in output from channel ϵ_{ox} for two anisotropic layers with $n_i=1$, $\epsilon_{Lx}=1.8$, $\epsilon_{Ly}=3.7$, $\epsilon_{Lz}=2.0$, $\epsilon_{ox}=3.0$, $\epsilon_{oy}=1.7$, $\epsilon_{oz}=2.0$. The crystal of the first layer is rotated by 40° around the z axis while the crystal of the material in output has the principal axis directed along the directions of the Cartesian axis. (a) gives the phase of the first ray in output. (b) represents the phase of the wave obtained as a sum of the first and the second traversal rays at output. (c) is represents the phase for the wave obtained as a sum of the first three rays at the output. (d) represents the phase of the output field with all the rays included for the structure.

bution of the third ray is so small that its influence on the final sum can be neglected. The last figure, Fig. 4(d), represents the phase of the whole output field from the structure, polarized along the x axis, and is substantially similar to Fig. 4(c). The matrix method applied to this example confirms the behavior shown in Fig. 4(d).

We now consider a periodic stack with ten periods (Fig. 5) formed with a unit cell composed of two birefringent layers with dielectric constants: $\epsilon_{1x}=3$, $\epsilon_{1y}=6$, $\epsilon_{1z}=4$ and $\epsilon_{2x}=7$, $\epsilon_{2y}=5$, $\epsilon_{2z}=4$, respectively. The thicknesses of the two layers are both $0.5 \mu\text{m}$. The input beam has a cylindrical Gaussian section (in the xy plane), the axis of the cylinder is the y axis. The beam propagates in a transversal way in the xz plane, the polarization is linear, normal to the beam and to the y axis. The input and output media are vacuum. The incidence angle

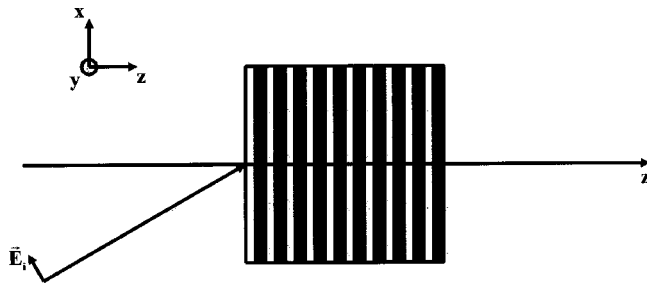


FIG. 5. Simple system that uses an anisotropic multilayer to create an anomalous phase in the output field. The periodic structure has ten periods, formed by two birefringent layers with dielectric constants: $\epsilon_{1x}=3$, $\epsilon_{1y}=6$, $\epsilon_{1z}=4$, $\epsilon_{2x}=7$, $\epsilon_{2y}=5$, $\epsilon_{2z}=4$, the thickness of the two layers are both $0.5 \mu\text{m}$, the wave in input is a beam with cylindrical section (on the xy plane) Gaussian, the axis of the cylinder is the y axis. The beam propagates in a transversal way on the xz plane; the polarization will be linear, normal to the beam and to the y axis. The input and output medium is vacuum. The incident angle is 30° with respect to the z axis. While the second crystal is rotated with respect to the first one by 30° around the z axis.

is 30° with respect to the z axis. The index axis of the first crystal is aligned to the reference frame (x, y, z) , while the second crystal is rotated with respect to the first one by 30° around the z axis. If we analyze the phase of the wave at the output in the channel ϵ_{ox} we obtain the graph of Fig. 6, which shows an anomalous phase in the range of the wavelengths from 0.520 to $0.522 \mu\text{m}$. The 30° value for optical axis's rotation is the value which maximize the anomalous phase for this specific example.

In what follows we present results obtained with the “ray” method and verified with the matrix method;¹⁷ more details of the numerical calculation in space and time are presented in this section are discussed in Appendix B.

To study the effects of the anomalous phase on the transverse structure of the input wave we fixed the wavelength of the beam at $\lambda=0.5207 \mu\text{m}$, thus inside the anomalous region. The input beam is a Gaussian beam with a finite spread

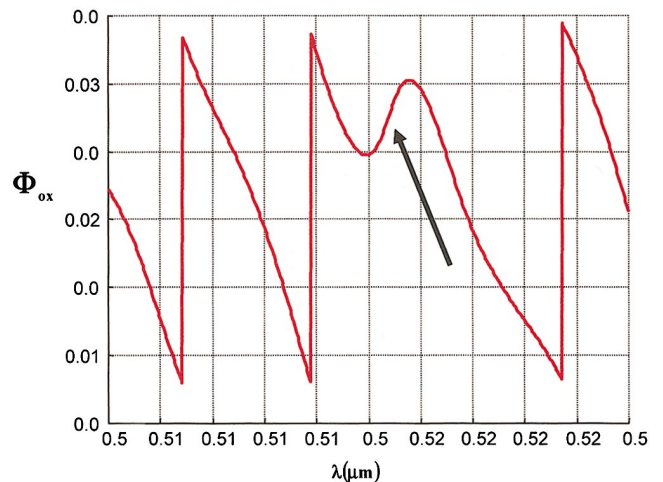


FIG. 6. (Color) The phase of the output wave in channel ϵ_{ox} , for the system of Fig. 5.

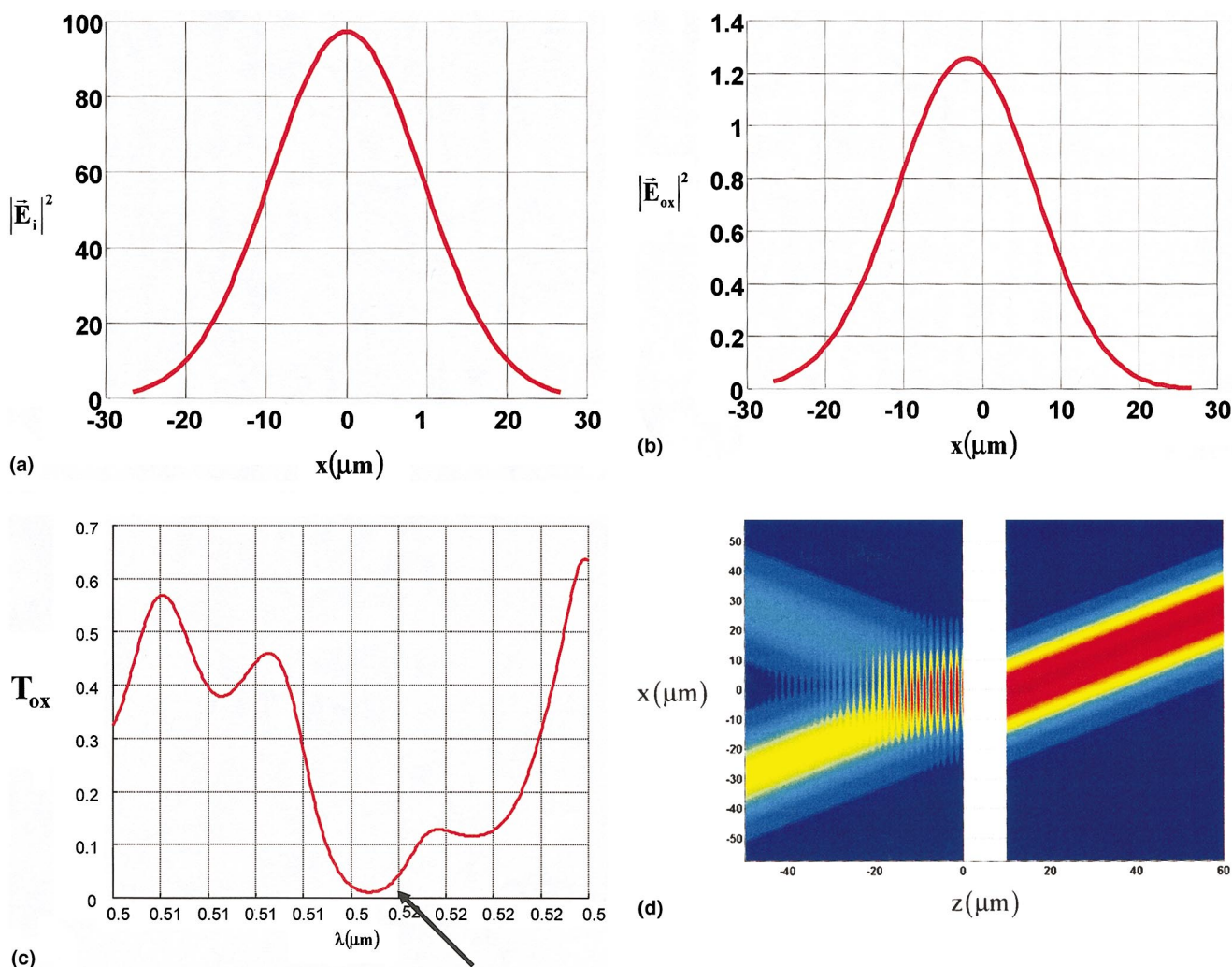


FIG. 7. (Color) Field behavior in channel ϵ_{ox} along the x axis for the case of Fig. 5 with a wavelength $\lambda=0.5207 \mu\text{m}$. (a) input Gaussian beam, (b) output Gaussian beam, (c) transmission spectrum of the multilayer, (d) intensity of incident, reflected, and transmitted beam: the output transmitted beam has been normalized to the transmission value in order to be visualized.

in the transverse wave vector k , that represents all the plane waves with the same wavelength $\lambda=0.5207 \mu\text{m}$. If the input Gaussian beam is sufficiently wide in space, the beam does not diffract and the spatial spectrum will be narrow enough to lie well within the range of the anomalous phase. As discussed in Appendix B, the output beam polarized in the plane xz undergoes an anomalous shift associated to the temporal shift of the wave front. In Fig. 7(a) the input field distribution on the x axis is shown, and Fig. 7(b) shows the shifted output field whose center has moved in the direction of the negative x . The output field amplitude is much smaller than the input field; Fig. 7(c) which shows the transmission of the structure. In Fig. 7(d) we show the intensity plot for incident, reflected, and transmitted polarized beam: the output transmitted beam is normalized to the transmission value for better visualization.

Now we analyze another example where we have an anisotropic multilayer structure with an anomalous phase in the spectrum and we show that an input pulse peak exits the structure before the entire wave has entered in the structure. This case is often called superluminal or photon tunneling

and the output pulse is described by negative times. We consider a periodic structure with *three* periods, everyone formed by two layers with the following dielectric constants: $\epsilon_{1x}=2$, $\epsilon_{1y}=4$, $\epsilon_{1z}=1$, and $\epsilon_{2x}=3$, $\epsilon_{2y}=6$, $\epsilon_{2z}=1$, respectively, the semispaces in input and output are the vacuum, while the second crystal is rotated of 45° with respect to the first one around the z axis, as represented in Fig. 3, where only two layers are shown. The thickness is $0.1 \mu\text{m}$ for the first layer and $0.17 \mu\text{m}$ for the second layer, the total thickness ($0.81 \mu\text{m}$) is much shorter than the width of the input Gaussian wave packet, given by

$$G(x,z,t) = e^{-x^2/(2\sigma_x^2)} e^{-(z-ct)^2/(2\sigma_z^2)}, \quad (11)$$

referring to the axes shown in Fig. 3. The origin of the axes is fixed at the entrance of the structure ($z=0$), and the beam moves along the z axis. We fix the constants in Eq. (11) as $\sigma_x=10 \mu\text{m}$, $\sigma_z=8.9437 \mu\text{m}$, and study the output wave at the time $t=0$. The calculation has been performed in the following way (details are presented in Appendix B): first we calculate at the $z=0$ plane, the Fourier transform of the input

pulse in the space and time domains; then we calculate the product of the transformed pulse with the transmission (as function of frequency and wave vector k); we apply the “propagator” in space; after that we calculate again the Fourier transform in space and time in the plane $z=z_0$ (where $z_0 \geq d$); and finally we get the field in $z=z_0$ and at the time $t=0$. In Fig. 8(a) the output phase along the x_2 -axis (axis x of the layer two) when in input we have a wave with linear polarization along the y_1 axis (axis y of the layer one) is shown. The dispersion plot in figure displays an anomalous phase band between the wavelengths $\lambda=0.52 \mu\text{m}$ and $\lambda=0.54 \mu\text{m}$. The central frequency of the Gaussian wave is $\lambda=0.53 \mu\text{m}$ and the entire range of principal frequencies of the Gaussian pulse is around the anomalous phase. The normalized to the transmission value output wave (in order to be visualized), together with the input pulse (it is visualized only the input and not the reflected pulse) and the space filled by the multilayer are shown in Fig. 8(b), where one can discern that the wave appears at the output before it enters the input. This, however, comes at a cost of a very low transmission energy. Note that we have normalized to unity the output wave because its amplitude is so low that one would not be able to see it on the same scale as the input field. We observe that no spatial distortion of the polarized beam occurs. In Fig. 8(c) we graph the amplitude of the transmission spectrum that put into evidence that in the range of the anomalous phase we need to have a low transmission to maintain the causality principle.

IV. CONCLUSIONS

We have shown that it is possible to construct an anisotropic, one-dimensional, multilayer geometry for which, in a given range of wavelengths and polarization, the phase of the transmitted field has a positive slope as a function of wavelength. This behavior is explained by adopting the simple ray method. Several specific examples are discussed for dielectric values not attributable to any specific material, however, realistic enough to demonstrate that birefringent layers introduce an anomalous phase that leads to anomalous shifts of the center of gravity of the beam, but with considerable reduction of the transmission coefficient. The anomalous phase results are obtained without the need to invoke contradictory refraction rules. A polarized beam propagating under conditions of anomalous phase travels through the structure without distortion provided its bandwidth lies within the anomalous dispersion region. Our numerical simulations confirm the results. Finally we note that the effect is already present in structures composed of only one layer over on an anisotropic semispace.

APPENDIX A

In this appendix we demonstrate the conditions under which the anomalous phase in one polarization is found in the output. We use as an example a structure built with two anisotropic layers with vacuum on the both sides, as represented in Fig. 3. We begin considering only the first ray that traverses through the structure (Fig. 3); from the figure it is

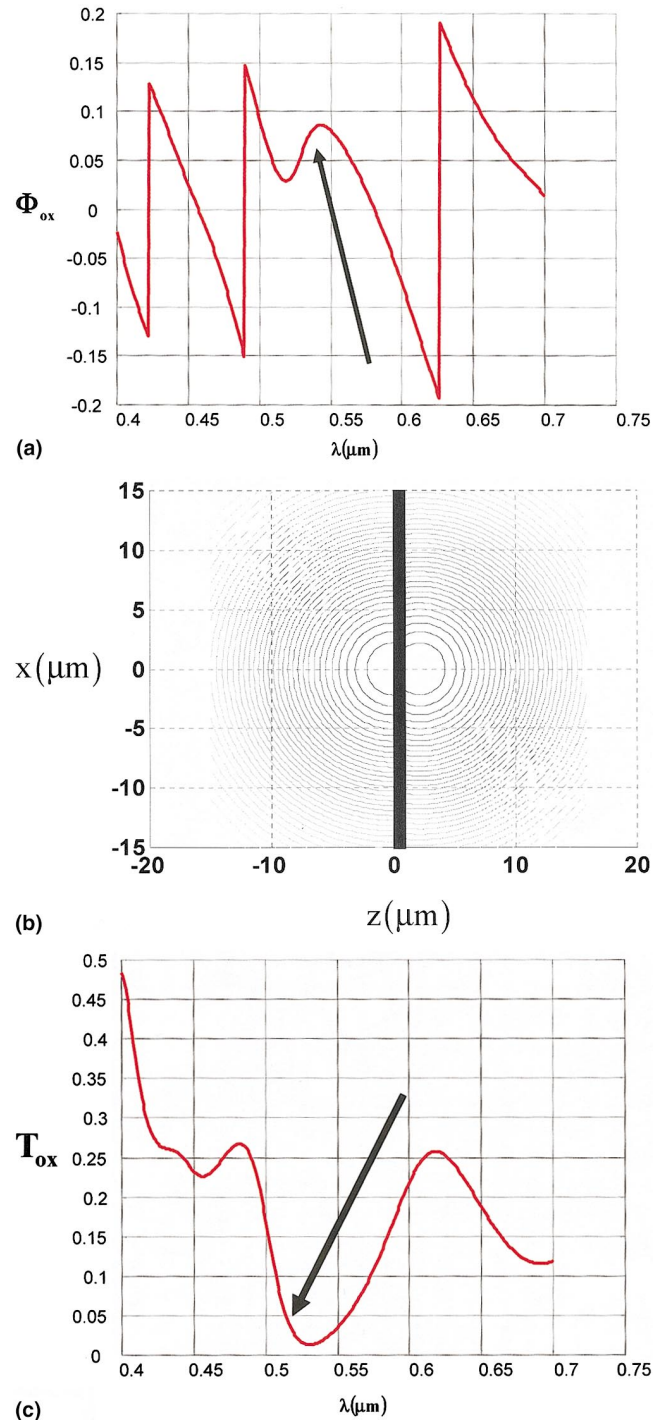


FIG. 8. (Color) Gaussian input wave in a multilayer structure. (a) Phase of the output. (b) Contour plot (amplitude) of the input and output wave in the propagation y - z plane within the middle the input space for the multilayer, the output has been normalized to the transmission, it has been plotted only the input pulse and not the reflected one. (c) Transmission spectrum.

clear that only at the interface between the two layers we can have the mix of energy between the two permitted channels of the two anisotropic layers and so obtain anomalous phase in the output wave.

If we study the output field behavior of the first ray that traverses the medium and the conditions under which this gives an anomalous phase, then we can extend these considerations to the total wave that includes a superposition of multiple rays at the output. Once we find the anomalous phase in the first-traversal ray, usually we have the same behavior in the total output field, because the other rays undergo reflections and have smaller amplitudes. So the first ray contributes the largest portion of energy of the total output wave.

Figure 3 depicts how the two layers are oriented. We maintain the same direction for the principal axis ε_{iz} ($i=a,b$) and rotate only around the z axis. The two rotations have the angles ϕ_a and ϕ_b for layer A and B , respectively. The plane wave in input is linear polarized with a rotation of the electric field round the z axis with value ϕ_p , it arrives at

the interface with normal incidence, so that the channels permitted by the anisotropic materials are those of the principal axis ε_{ix} and ε_{iy} ($i=a,b$). We can write the expression for the first ray in output as

$$\vec{E}_{o1} = \alpha_{bo}\Delta_b\alpha_{ab}\Delta_a\alpha_{ia}\begin{pmatrix} \cos(\phi_p) \\ \sin(\phi_p) \end{pmatrix}. \quad (A1)$$

This is a vector because we have two polarizations in output for the two channels of the second layer. We can expand formula (A1) and obtain the analytical expression for the field along the x_o axis that we choose with the same direction of the x_b axis. So we obtain

$$E_{tx} = e^{(2i\pi d_b n_{bx})/\lambda} (Ae^{(2i\pi d_a n_{ax})/\lambda} + Be^{(2i\pi d_a n_{ay})/\lambda}), \quad (A2)$$

with the coefficients A and B written as

$$A = \frac{8\text{Cos}[\phi_a - \phi_b]\text{Cos}[\phi_p]n_{ax}n_{bx}(n_{ay} + n_{by})}{(1 + n_{ax})(1 + n_{bx})\{\text{Sin}[\phi_a - \phi_b]^2 n_{ay}n_{by} + n_{bx}(\text{Cos}[\phi_a - \phi_b]^2 n_{ay} + n_{by}) + n_{ax}(n_{ay} + \text{Sin}[\phi_a - \phi_b]^2 n_{bx} + \text{Cos}[\phi_a - \phi_b]^2 n_{by})\}}$$

$$B = \frac{-8\text{Sin}[\phi_a - \phi_b]\text{Sin}[\phi_p]n_{ay}n_{bx}(n_{ax} + n_{by})}{(1 + n_{ay})(1 + n_{bx})\{\text{Sin}[\phi_a - \phi_b]^2 n_{ay}n_{by} + n_{bx}(\text{Cos}[\phi_a - \phi_b]^2 n_{ay} + n_{by}) + n_{ax}(n_{ay} + \text{Sin}[\phi_a - \phi_b]^2 n_{bx} + \text{Cos}[\phi_a - \phi_b]^2 n_{by})\}} \quad (A3)$$

Eq. (A1) can be written as

$$E_{tx} = Ae^{i(\alpha/\lambda)} + Be^{i(\beta/\lambda)}, \quad (A4)$$

where α and β are given by

$$\alpha = 2\pi\left(\frac{d_a n_{ax} + d_b n_{bx}}{d_a + d_b}\right)(d_a + d_b)$$

$$\beta = 2\pi\left(\frac{d_a n_{ay} + d_b n_{bx}}{d_a + d_b}\right)(d_a + d_b). \quad (A5)$$

If we want to find the anomalous phase in the output field due to the first-traversal ray, we need to calculate the phase of Eq. (A4). If an anomalous region exists for the phase, the function must have a maximum and minimum, so we have to search for these points.

To find the stationary points in the phase function we can observe that for the arctangent function we may write

$$\frac{d}{d\lambda} \text{tg}^{-1}(f) = \frac{1}{1 + f(x)^2} \frac{df}{d\lambda}. \quad (A6)$$

The stationary points for the arctangent are the same of those of the function that is in the argument. To calculate the stationary points of the phase of Eq. (A4) we can calculate the function $f = [\text{Im}(f)]/\text{Re}(f)$ of Eq. (A4) and apply Eq. (A6). So we have

$$f = \frac{A\text{Sin}\left[\frac{\alpha}{\lambda}\right] + B\text{Sin}\left[\frac{\beta}{\lambda}\right]}{A\text{Cos}\left[\frac{\alpha}{\lambda}\right] + B\text{Cos}\left[\frac{\beta}{\lambda}\right]}, \quad (A7)$$

and

$$\frac{df}{d\lambda} = -\frac{A^2\alpha + B^2\beta + AB(\alpha + \beta)\text{Cos}\left[\frac{\alpha - \beta}{\lambda}\right]}{\lambda^2\left(A\text{Cos}\left[\frac{\alpha}{\lambda}\right] + B\text{Cos}\left[\frac{\beta}{\lambda}\right]\right)^2}. \quad (A8)$$

Imposing the condition $df/d\lambda=0$ we have the solutions

$$\lambda = \frac{(\alpha - \beta)}{\text{Arccos}\left[\frac{-A^2\alpha - B^2\beta}{AB(\alpha + \beta)}\right] + 2n\pi} \quad n \in \mathbb{Z}. \quad (A9)$$

To have solutions in the real space it is necessary that the argument inside the arc cosine is smaller than +1 and bigger than -1.

$$-1 < \frac{-A^2\alpha - B^2\beta}{AB(\alpha + \beta)} < 1. \quad (A10)$$

This condition set all parameters whose values contribute to the definition of ‘‘anomalous phase region.’’ We can expand the expression of the arccosine’s argument to obtain

$$\begin{aligned}
\frac{-A^2\alpha - B^2\beta}{AB(\alpha + \beta)} = & (16\text{Cos}[\phi_a - \phi_b]\text{Cos}[\phi_p]\text{Csc}[2(\phi_a - \phi_b)]^2\text{Csc}[2\phi_p]^2\text{Sin}[\phi_a - \phi_b]\text{Sin}[\phi_p]) \\
& \times \{d_a[\text{Cos}[\phi_a - \phi_b]^2\text{Cos}[\phi_p]^2n_{ax}^3n_{ay}^4 + \text{Cos}[\phi_a - \phi_b]^2\text{Cos}[\phi_p]^2n_{ax}^3n_{by}^2 \\
& + 2\text{Cos}[\phi_a - \phi_b]^2\text{Cos}[\phi_p]^2n_{ax}^3n_{ay}n_{by}(1 + n_{by}) \\
& + \text{Cos}[\phi_a - \phi_b]^2\text{Cos}[\phi_p]^2n_{ax}^3n_{ay}^2[1 + n_{by}(4 + n_{by})] \\
& + n_{ay}^3\text{Sin}[\phi_a - \phi_b]^2\text{Sin}[\phi_p]^2n_{ax}^4 + \text{Sin}[\phi_a - \phi_b]^2\text{Sin}[\phi_p]^2n_{by}^2 + \{1 + \text{Cos}[2(\phi_a - \phi_b)]\text{Cos}[2\phi_p]n_{ax}^3(1 + n_{by}) \\
& + 2\text{Sin}[\phi_a - \phi_b]^2\text{Sin}[\phi_p]^2n_{ax}n_{by}(1 + n_{by}) + \text{Sin}[\phi_a - \phi_b]^2\text{Sin}[\phi_p]^2n_{ax}^2(1 + n_{by}(4 + n_{by}))\}] \\
& + d_bn_{bx}[\text{Sin}[\phi_a - \phi_b]^2\text{Sin}[\phi_p]^2n_{ax}^4n_{ay}^2 + \text{Sin}[\phi_a - \phi_b]^2\text{Sin}[\phi_p]^2n_{ay}^2n_{by}^2 + 2\text{Sin}[\phi_a - \phi_b]^2\text{Sin}[\phi_p]^2n_{ax}^3n_{ay}^2(1 + n_{by}) \\
& + 2\text{Sin}[\phi_a - \phi_b]^2\text{Sin}[\phi_p]^2n_{ax}n_{ay}^2n_{by}(1 + n_{by}) \\
& + n_{ax}^2(\text{Cos}[\phi_a - \phi_b]^2\text{Cos}[\phi_p]^2n_{ay}^4 + \text{Cos}[\phi_a - \phi_b]^2\text{Cos}[\phi_p]^2n_{by}^2 \\
& + 2\text{Cos}[\phi_a - \phi_b]^2\text{Cos}[\phi_p]^2n_{ay}^3(1 + n_{by}) + 2\text{Cos}[\phi_a - \phi_b]^2\text{Cos}[\phi_p]^2n_{ay}n_{by}(1 + n_{by}) + \frac{1}{2}\{1 + \text{Cos}[2(\phi_a \\
& - \phi_b)]\text{Cos}[2\phi_p]\}n_{ay}^2[1 + n_{by}(4 + n_{by})]]\}] \\
& /n_{ax}(1 + n_{ax})n_{ay}(1 + n_{ay})[d_a(n_{ax} + n_{ay}) + 2d_bn_{bx}](n_{ax} + n_{by})(n_{ay} + n_{by}). \tag{A11}
\end{aligned}$$

Equation (A11) is not simple but it gives the analytical expression and the conditions to generate anomalous phase in the system, as a function of the physical parameters of the geometry, such as refraction indexes, polarization of the input plane wave, thickness of the two layers, and the relative rotation of the two crystals of the corresponding layers, therefore a suitably selection of the above mentioned parameters allows the geometry to manifest “anomalous phase” for the transmission function.

APPENDIX B

The numerical calculations presented as examples have been performed adopting the following method. Let us consider a medium of extension d , along the z axis (as in Fig. 1 and in Fig. 3), with an input surface at $z=0$, and output surface at $z=d$, and an input polarized field whose scalar amplitude is $V(x, y, z=0, t)$ traveling along the z axis. The field on the output surface will be $V(x, y, d, t)$. For a linear medium we can apply the Fourier analysis at $z=0$ and $z=d$, respectively, so that

$$\begin{aligned}
V(k_x, k_y, z=0, \omega) &= \int_{-\infty}^{\infty} \int_{-\infty}^{\infty} \int_{-\infty}^{\infty} V(x, y, z \\
&= 0, t) e^{i(\omega t - k_x x - k_y y)} d\omega dx dy, \tag{B1a}
\end{aligned}$$

and

$$\begin{aligned}
V(k_x, k_y, z=d, \omega) &= \int_{-\infty}^{\infty} \int_{-\infty}^{\infty} \int_{-\infty}^{\infty} V(x, y, z \\
&= d, t) e^{i(\omega t - k_x x - k_y y)} d\omega dx dy. \tag{B1b}
\end{aligned}$$

The transfer matrix method set the link between output and input field

$$V(k_x, k_y, z=d, \omega) = T(k_x, k_y, \omega) V(k_x, k_y, z=0, \omega), \tag{B2}$$

where the complex function $T(k_x, k_y, \omega)$ contains all the information on the geometry of the structure. Then the output field is obtained performing the inverse Fourier transform in the space-time domain.

Now let us consider a paraxial input field; if the transmission $T(k_x, k_y, \omega)$ for a first approximation and for a specific range of frequencies can be written as $T(k_x, k_y, \omega) = |T|e^{i\varphi}$, $|T|$ being constant, one may expand the phase in a Taylor series around specific values of ω and k : $T(k_x, k_y, \omega) = |T|e^{i(\varphi_0 + \delta\phi)}$. Retaining only the first term of the phase expansion, we have

$$\begin{aligned}
V(k_x, k_y, z=d, \omega) &= V(k_x, k_y, z=0, \omega) T(k_x, k_y, \omega) \\
&\cong V(k_x, k_y, z=0, \omega) T_0 e^{+i\alpha\omega}, \tag{B3}
\end{aligned}$$

α being the slope of the phase in the spectral region of interest and $T_0 = |T|e^{i\varphi_0}$. With this hypothesis, the output field in the time domain will be

$$\begin{aligned}
V(k_x, k_y, z=d, t) &= \int_{-\infty}^{\infty} V(k_x, k_y, z=0, \omega) T_0 e^{+i\alpha\omega} e^{-i\omega t} d\omega \\
&= T_0 V(k_x, k_y, z=0, t - \alpha). \tag{B4}
\end{aligned}$$

So the output field is simply related to the field in input, but shifted in time (i.e., advanced or delayed) depending on the slope of the phase and with the amplitude scaled by the value of the transmission coefficient T_0 . By applying again the Fourier transform on the transverse k components, we have finally the expression of the output field given by

$$V(x, y, z = d, t) = \int_{-\infty}^{\infty} \int_{-\infty}^{\infty} T_0 V(k_x, k_y, z = 0, t - \alpha) e^{i(k_x x + k_y y)} dk_x dk_y$$

$$= T_0 V(x, y, z = 0, t - \alpha). \quad (\text{B5})$$

The output field at $z=d$ is equal, with a scale factor T_0 , to the input field in $z=0$, only if $\alpha=0$, otherwise on the output surface we will have the same input field suitably shifted in time: delayed if $\alpha>0$, or advanced if $\alpha<0$. Then when an anomalous phase occurs we obtain an output wave that is simply a copy of the input field, with a superluminal time shift depending on the phase slope and with the amplitude scaled by the transmission coefficient value.

We present now a simple picture enabling us to compute the lateral shift of the beam. For the sake of clarity we will treat only a two-dimensional problem and neglect the y dependence. In order to compute the lateral shift, we need to compare the beam finite profile of both the output transmitted beam and the incident beam wave in the plane $x-z$ at $z=d$ and $z=0$ at $t=0$ [Fig. 9(a)]. Let us consider an input beam of Gaussian shape $V_n(x, z, t) = e^{-(x^2)/2\sigma_x^2} e^{i(\omega_0 t - kz)}$ impinging on the input surface in the $x-z$ plane with a certain angle φ

$$V(x', z', t) = e^{-[(-z' \sin \varphi + x' \cos \varphi)^2]/2\sigma_x^2} e^{i(\omega_0 t - z' k \cos \varphi - x' k \sin \varphi)}$$

being $\begin{cases} z = z' \cos \varphi + x' \sin \varphi \\ x = -z' \sin \varphi + x' \cos \varphi \end{cases}$

If we name z' as z and x' as x we have

$$V(x, z, t) = e^{-[(-z \sin \varphi + x \cos \varphi)^2]/2\sigma_x^2} e^{i(\omega t - z k \cos \varphi - x k \sin \varphi)}, \quad (\text{B5a})$$

assuming $k_x = k \sin \varphi$ and $k_z = k \cos \varphi$ and redefining a new $\sigma^2 = \sigma_x^2 k^2$, we can represent Eq. (B5a) as

$$V(x, z, t) = G(k_z x - k_x z) e^{i(\omega t - k_x x - k_z z)}, \quad (\text{B6})$$

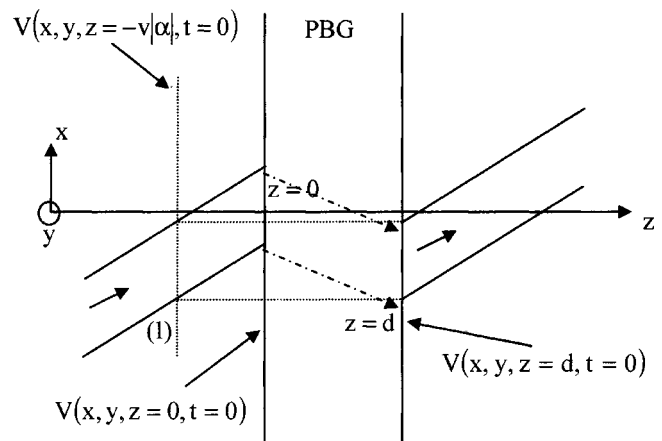
where G is the Gaussian function $G(k_z x - k_x z) = e^{[-(k_z x - k_x z)^2]/2\sigma^2}$. By adopting the same calculation presented before, we have the input beam at $z=0$ and $t=0$ as

$$V(x, z = 0, t = 0) = G(k_z x) e^{-ik_x x}. \quad (\text{B7})$$

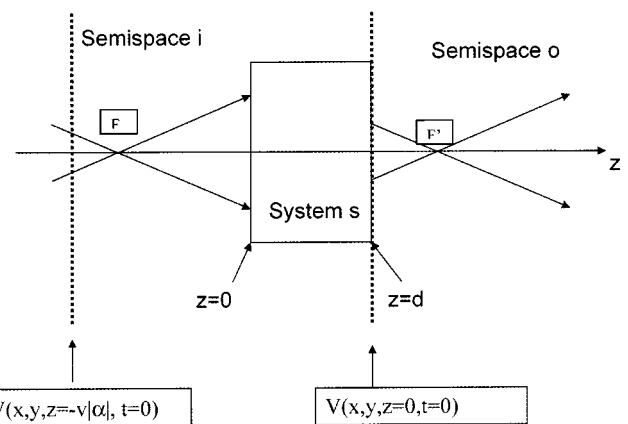
Under the same hypothesis presented before, i.e., with a phase of the transmission represented in terms of a series expansion around k and with a linear slope, after some algebra, at time $t=0$ we have the field at the $z=d$ interface given by

$$V(x, z = d, t = 0) = T_0 V(x, z = v\alpha, t = 0) = T_0 G(k_z x - k_x v\alpha) e^{-i(k_x x + k_z v\alpha)} = T_0 G(k_z x - k_x v\alpha) e^{-ik_x x} e^{-ik_z v\alpha}, \quad (\text{B8})$$

where v is the phase velocity, we have that Eq. (B8) is the same as Eq. (B7) with a spatial shift $k_x v\alpha/k_z$ along the x axis of the Gaussian field envelope. This is the amount of spatial shift of the beam along x axis produced by the linear phase dispersion of the geometry.



(a)



(b)

FIG. 9. (a) Graphical representation of the later spatial shift in the $x-z$ plane in the case of anomalous phase. (b) Graphical representation of the refraction of an extended and focalized for an anomalous phase of the transmission of the geometry (named system s), equivalent to the one expected for a “negative refractive index” material.

We can conclude that, due to the temporal translation introduced by the medium dispersion, we have an equivalent spatial translation of the beam along the x axis whose amplitude depends on d and on α , i.e., towards the top or bottom of the axis depending on the sign of α : toward the top of the x axis for $\alpha>0$, and towards the bottom for $\alpha<0$ (anomalous phase region as plotted in Fig. 5). This spatial translation does not contradict Snell’s law (the plane wave never undergoes a negative refraction in order to be on the same side of the normal at the interface as the incident beam) and the usual refraction laws, only introduce an “apparent” negative refraction associated to the temporal and spatial translation of the beam [see Fig. 9 where we consider a PBG (photonic band gap or multilayer) medium whose refraction is anomalous, according to the properties of the phase of the transmission as discussed before; the dotted arrows simulate the ray trajectory in “negative refractive index medium,” this is just a graphical representation of the Fig. 7(d), where the reflected field has been omitted].

The consequence can be summarized in Fig. 9(b): for a system with anomalous phase in the paraxial limit, if we

consider a focused beam along the z axis (F is the focus), the front phase surface at $t=0$ and at $z=-|\alpha|v$ will be found at $z=d$ and at $t=0$, with an amplitude modified by the PBG transmission, all waves on the right side of the front phase surface $t=0$ and at $z=-|\alpha|v$, will be found on the right side

of the surface $z=d$; the focal point F' is produced in the same way as in the case of a “negative refractive index” medium. The plot is just a graphical representation and not a result of a numerical simulation therefore any reflected field has been omitted.

*FAX: +39 06 442 40 183. Electronic address: concita.sibilia@uniroma1.it

¹M. Gerken and D. A. B. Miller, *Appl. Opt.* **42**, 1330 (2003).

²H. Kosaka, T. Kawashima, A. Tomita, M. Notomi, T. Tamamura, T. Sato, and S. Kawakami, *Phys. Rev. B* **58**, R10096 (1998).

³E. Yablonovitch, *Phys. Rev. Lett.* **58**, 2059 (1987).

⁴S. John, *Phys. Rev. Lett.* **58**, 2486 (1987).

⁵J. D. Joannopoulos, R. D. Meade, and J. N. Winn, *Photonic Crystals: Molding the Flow of Light* (Princeton University Press, Princeton, NJ, 1995).

⁶M. Notomi, *Phys. Rev. B* **62**, 10 696 (2000).

⁷C. Luo, S. G. Johnson, J. D. Joannopoulos, and J. B. Pendry, *Phys. Rev. B* **65**, 201104 (2002).

⁸C. Luo, S. G. Johnson, and J. D. Joannopoulos, *Appl. Phys. Lett.* **81**, 2352 (2002).

⁹V. G. Veselago, *Usp. Fiz. Nauk* **92**, 517 (1968) [*Sov. Phys. Usp.* **10**, 509 (1968)].

¹⁰J. B. Pendry, *Phys. Rev. Lett.* **85**, 3966 (2000).

¹¹R. A. Shelby, D. R. Smith, and S. Schultz, *Science* **292**, 77 (2001).

¹²C. Luo, S. G. Johnson, J. D. Joannopoulos, and J. B. Pendry, *Opt. Express* **11**, 746 (2003).

¹³S. Foteinopoulou, E. N. Economou, and C. M. Soukoulis, *Phys. Rev. Lett.* **90**, 107402 (2003).

¹⁴Y. Zhang, B. Fluegel, and A. Mascarenhas, *Phys. Rev. Lett.* **91**, 157404 (2003).

¹⁵A. Mandatori, C. Sibilia, M. Centini, G. D’Aguanno, M. Bertolotti, M. Scalora, M. Bloemer, and C. M. Bowden, *J. Opt. Soc. Am. B* **20**, 504 (2003).

¹⁶M. Born and E. Wolf, *Principles of Optics* (Pergamon Press, Oxford, 1965).

¹⁷P. Yeh and A. Yariv, *Optical Waves in Layered Media* (Wiley, New York, 1988).